

Monika Srivastava<sup>1\*</sup>, Ikhwan Syafiq Mohd Noor<sup>2</sup>,  
Muhd Zu Azhan Yahya<sup>3</sup>, R. C. Singh<sup>1</sup>

<sup>1</sup>Centre for Solar Cell and Renewable Energy, Department of Physics, Sharda University, Greater Noida, India, <sup>2</sup>Physics Division, Centre of Foundation Studies for Agricultural Sciences, Universiti Putra Malaysia, UPM Serdang, 43400, Selangor Darul Ehsan, Malaysia, <sup>3</sup>Muhd Zu Azhan Yahya Faculty of Defence Science and Technology, Universiti Petrahanan Nasional Malaysia (UPNM), Kuala Lumpur, Malaysi

Scientific paper

ISSN 0351-9465, E-ISSN 2466-2585

<https://doi.org/10.62638/ZasMat1257>



Zastita Materijala 65 (4)  
690 - 702 (2024)

## Synthesis and scalable process for fabrication of Perovskite Solar Cells using organic and inorganic hole transport materials

### ABSTRACT

*The Organic Inorganic Lead Iodideperovskite material has emerged as a pioneer in being an active material for third generation solar cells. Apart from the synthesis, the scalable mechanism which is being used for the deposition process, greatly influences the performance of the cell owing to its impact on the morphology, uniform thickness and interface between two functional layers. This study briefly discusses the various deposition processes involved in assembling the layers of perovskite solar cells (PSC). Hole transport materials (HTM) are the crucial part of the PSC providing efficient transport of the charge carriers. However the effect of organic and inorganic HTMs is highly pronounced in the PSCs. This study also discusses the effect of organic and inorganic HTM on the stability and efficiency of the sandwich structured PSC.*

**Keywords:** Perovskite, Solar energy, PCE, Hole transport material

### 1. INTRODUCTION

As we know that across the world the energy consumption is continuously increasing and is estimated to elevate by approximately 48% by the end of 2040, as stated by Energy Information Administration (EIA, 2015). This surge in the energy consumption is primarily due to growth in population and living standard of the people which translates into greater use of energy products. Clean and renewable energy sources are needed to dominate this domain for sustainable developments (McGeoch *et al.*, 2010). Solar cells are the effective way to harness the sun's energy to convert it into electricity and thus provide the opportunity to overcome humanity's continued increase in demand and consumption of available energy (Service, 2005). Compared to other means, for example photochemical reaction and solar thermal, solar cells offer an efficient and safer way to meet the energy demands across the globe. However, it has the capacity to efficiently transport and store energy. Thus, the main aim of this technology is to use solar energy in the most efficient way.

In 1954, the first known silicon solar cell was fabricated at Bell laboratories. The solar cell achieved an efficiency of 6%. Three generations of solar cells are under development in 60 years, based on the device engineering and the fundamental understanding of these photovoltaics. Silicon based solar cells that achieve efficiency as high as 26%, also classified as of the first generation, are the most successful commercially. The second generation of photovoltaics includes thin film solar cell technologies such as Copper Indium Gallium Selenide (CIGS), Cadmium Telluride (CdTe), and Gallium Arsenide (GaAs) also shows promising efficiencies. Gallium arsenide solar cells show a record efficiency of 29.3% under solar illumination condition (Polman *et al.*, 2016). But due to scarcity and toxicity of second generation, the third generation, have emerged, which includes the organic solar cells (OSC), Dye Sensitized Solar Cells (DSSC) and Perovskite Solar Cells (PSC) (Sengul and Theis, 2011; Gratzel, 2009). The third generation of solar cell technology is commonly known as an emerging generation of technologies. It encompasses a diverse array of solar cells that exhibit enhanced photovoltaic characteristics. These solar cells are characterized by their affordability, solution-based processing, and straightforward manufacturing processes that do not compromise their efficiency (Roy *et al.*, 2022).

The metal halide based perovskites have proved themselves as a promising photovoltaic

\*Corresponding author: Monika Srivastava

E-mail: [monika.srivastava@sharda.ac.in](mailto:monika.srivastava@sharda.ac.in)

Paper received: 07.03.2024.

Paper corrected: 23.05.2024.

Paper accepted: 06.06.2024.

material in the photovoltaic applications. The term 'Perovskite' follows the same crystal structure as  $\text{CaTiO}_3$  and they are expressed as  $\text{ABX}_3$ , where 'A' is the methyl ammonium (organic) cation, 'B' is the Pb cation and X is the halide ion. These cations and anions can be easily changed to tune the bandgap of the perovskite material. The metal halide perovskites have a number of applications for photovoltaic devices, Light emitting diodes, sensors etc. the year 2009 marks the first demonstration of a PSC with an efficiency of 3.8% (Kojima et al., 2009). This work garnered the interest of the scientific community towards the high absorption coefficient of PSCs. However the initial reported works were based on the liquid electrolyte PSC, therefore it leads to the leakage of the electrolyte causing low efficiency and instability. However, the year 2012, was a breakthrough in the area of PSCs which uses the HTM instead of the liquid electrolyte for the fabrication purpose. This increases the (PCE) efficiency of the PSC upto 10% (Kim et al., 2012; Lee et al; 2012). However, with certain modifications, the PCE of the perovskite solar cells have obtained an efficiency of ~ 25.4% within a duration of 10 years. It is discussed in this paper about the recent progress in the fabrication of PSCs and focus on the challenges which are faced for its commercialization. Perovskite solar cells (PSCs) boast several benefits, including their lightweight nature, adjustable bandgap of the sensitizer material, ease of production, and scalability. However, despite their potential, they are still in the early stages of industrialization compared to other solar technologies. A significant challenge is that efficient PSCs often use gold (Au) as an electrode, which adds to the cost of the devices. Finding a low-cost alternative for the electrode could mitigate

this issue. Additionally, most top-performing PSCs are based on lead (Pb), which introduces concerns about toxicity. Efforts are underway to find non-toxic alternatives to Pb, yet no Pb-free PSC has surpassed the performance of Pb-based counterparts so far. The scientific community continues to explore alternatives to eliminate the toxicity issue. Substances like Sn, Rb, Ge, Bi, and antimony (Sb) have been identified as potential candidates for creating toxin free metal halide perovskite materials. Among these, Sn has shown the most promising performance in PSCs. However the Sn based PSC were not able to attain the efficiency and stability of Pb based PSCs. This may be due to oxidation of Sn and also poor band matching between the perovskite, ETL and HTL. Nishimura et al., addressed this problem by partially substituting formamidium ion with ethyl ammonium ion which enhances the photo conversion efficiency of the PSC to 13%. Min et al., took a completely different approach where an interface layer was introduced between the ETL and the Perovskite layer which eliminated the need of surface passivation. With this modification, the PSC attained an efficiency of 25.5% with retention of 90% efficiency even after 500 h.

### 1.2 Structure of the Perovskites:

The organic-inorganic lead iodide perovskite material has a general formula of  $\text{ABX}_3$ . In this, the cations "A" and "B" are occupied at the cubic and octahedral sites, respectively, where X can be any of the following: oxygen, carbon, nitrogen, or halogen. The cation 'A' is placed at cubic octahedral site and the cation B is occupied at the octahedral site, where (X = oxygen or halogen).

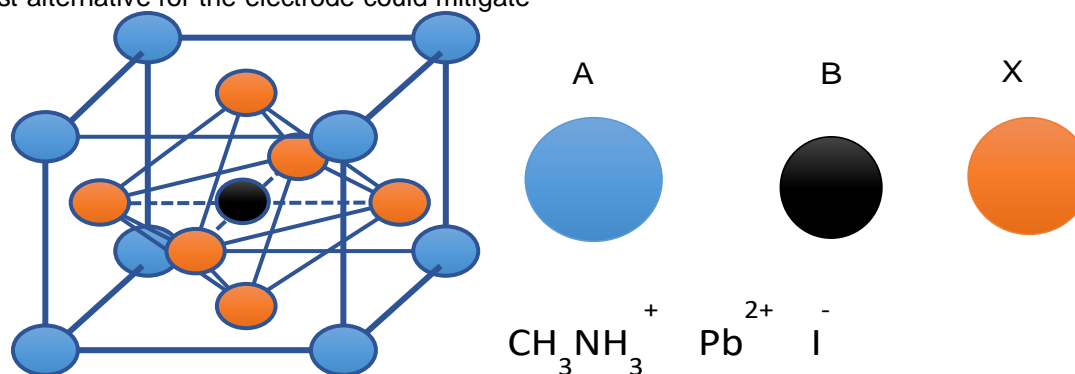


Figure 1: Structure of  $\text{MAPbI}_3$

Thus the charge neutrality is achieved by the monovalent A and divalent B cations through the perovskite holding halogen anions. Methyl Ammonium lead iodide ( $\text{MAPbI}_3$ ) has extraordinary optical and electronic characteristics (Baikie et al., 2013) where the band gap is 1.58 eV and an absorption which starts from 800 nm and is having

high absorption coefficient. The  $\text{MAPbI}_3$  has low binding energy of 50 meV which results in easy generation of the excitons even at room temperature (Ponseca et al., 2015). Therefore, the excitons which are generated exhibit a display of small masses bringing about high transporter mobilities of  $27 \pm 7 \text{ cm}^2 \text{ V}^{-1}\text{s}^{-1}$  for electrons and

$105 \pm 3 \text{ cm}^2 \text{ V}^{-1} \text{ s}^{-1}$  for holes. In addition excitons produced have a long diffusion length around 100 nm to 1000 nm. (Dong et al., 2015, Assadi et al., 2018).

## 2. SCALABLE TECHNIQUES FOR THE PSC

### 2.1. Vacuum Deposition:

In the year 1999, Mitzi et al., were the first one to use vacuum deposition in which organic inorganic compounds were deposited on a substrate. This technique controls the film composition and thickness giving high reproducibility. Snaith et al., used this technique to deposit  $\text{MAPbI}_3$  to obtain excellent uniformity of the film, thus obtained an efficiency of 15% (Liu et al., 2013). The previous works suggests that the

perovskite film deposited with the help of vapour deposition method give considerably improved efficiency. Since this technique is free from any toxic solvent therefore it still holds its importance in the field even though the process is expensive (Fig. 2 A). Recent advancements in vacuum deposition techniques have significantly benefited the development of perovskite materials, including those with mixed halides (Longo et al., 2018), low bandgap properties (Iguar-Muñoz et al., 2020), and formamidinium-based PSCs (Chiang et al., 2020; Feng et al., 2021). Notably, a peak efficiency of 21.32% was achieved in small-size cells (Feng et al., 2021), and 18.13% efficiency was reported for mini-modules with  $21 \text{ cm}^2$  as an effective device area (Li J. et al., 2020).

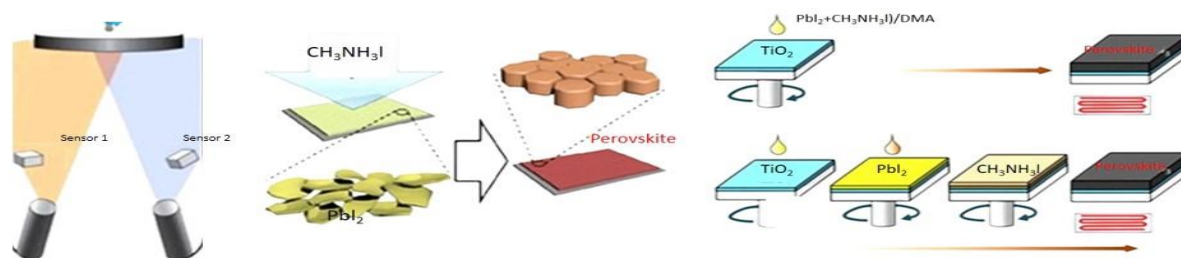


Figure 2. (A) Vacuum Deposition of Perovskite material (B) Vapour Deposition of perovskite material. (C) Deposition methods (One step and two step) of perovskite material.

### 2.2. One step deposition

The one step deposition method is a solution processed method which is favourably used for the deposition of perovskite layer on the substrate. In this method the precursor is prepared by mixing Methyl ammonium iodide (MAI) and lead iodide ( $\text{PbI}_2$ ) in N,N-Dimethyl formamide (DMF) with continuous stirring at  $60^\circ\text{C}$  for 6 hours. The prepared solution is spin coated on the substrate to obtain a uniform thickness (Fig. 2C). The Perovskite layer coated is then kept on the hot plate for 30 minutes at  $70^\circ\text{C}$  to evaporate the solvent. This method is simple to be conducted in laboratory. However, in order to obtain compact and pinhole free perovskite layer, this process is followed by applying the antisolvent on the functional layer. The antisolvents generally used are toluene (Jeon et al., 2014), chlorobenzene (Bi et al., 2016) and diethyl ether (Gao et al., 2018), fullerene (Wu et al., 2016). Some researchers have reported that polymer dissolved in antisolvents reduce the trap sites and non radiative recombination loss (Quin et al., 2018).

### 2.3. Two Step deposition Method

This method is also a very commonly used for deposition of perovskite materials to ease the reproducibility process. In this method, at first the

substrate is coated with  $\text{PbI}_2$  solution through spin coating and then MAI solution is coated on it. In another process of two step deposition, the MAI is applied by dip coating on the  $\text{PbI}_2$  coated substrate for 20 Sec. The two step deposition method has a better film morphology and give more efficient PSCs as compared to one step deposition method (Srivastava et al., 2021) (Fig. 2 C). However this process has a limitation of conversion of  $\text{PbI}_2$  to Perovskite, thus leading to poor efficiency and stability of the PSC (Chiang et al., 2017; Xu et al., 2019). These unconverted  $\text{PbI}_2$  often lead to the degradation of the PSC and also impedes the carrier transportation. (Jiang et al., 2016).

### 2.4. Vapour Assisted Deposition Method

As compared to other processes the vapour deposited perovskite film demonstrate a superior uniformity and thus resulting in better performance of the solar cell (fig 2 B). One clear benefit of using vapor deposition compared to solution processing is the capability to create multi-layered thin films across extensive surfaces. Vapor deposition is an established method employed in various sectors, including the glazing, liquid-crystal display, and thin-film solar cell industries. This technique enables the precise optimization of electronic contacts at interfaces by applying multilayers that have specific doping levels, as seen in the

crystalline silicon 'heterojunction with thin intrinsic layer' solar cells and in thin-film solar cells. Furthermore, this method is also applied in the development of organic light-emitting diodes. One of the studies uses vapour deposition of  $\text{PbI}_2$  followed by blade coating of perovskite solution. This method avoids the use of toxic solvents and also is efficiently applicable for large area PSCs (Zhang et al., 2024). In addition, the interface recombination and regulated of perovskite crystallization is achieved by introduction of urea additives.

Not only the deposition of the perovskite layer affects the efficiency of the PSC but also the process applied for the deposition of other functional layers such as HTM and Electron transport layer affects the performance of the cell. In one of the recent study the performance of the solar cell is enhanced and also the cost of fabrication is reduced by depositing thin  $\text{TiO}_2$  films (ETL) by sputtering method without thermal at ambient temperature. When compared to thermally sintered  $\text{TiO}_2$  films, the sputtered films showed advantages in carrier concentration, electron mobility, and hole-blocking capabilities along with well-matched band alignment and defect reduction with appropriate UV treatment (Yoo et al., 2024). There are certain other wide band gap materials

which are used as ETL other than  $\text{TiO}_2$  such as  $\text{ZnO}$  and  $\text{SnO}_2$ . In one of the studies, the ETL  $\text{SnO}_2$  is modified by adding non-ionic polymeric polyacrylamide (PAM) which prevents the formation of clusters in the  $\text{SnO}_2$  layer that improves the efficiency by reaching a PCE of 21.61% (Chen et al., 2024).

### 3. SANDWICHED STRUCTURED PEROVSKITE SOLAR CELLS

There has been a number of works in the area of sandwich structured PSCs. At first Park et al., worked on the sandwich based perovskite solar cells on the same structure as the DSSC only the Dye was replaced by perovskite sensitizer. Using this sensitization concept the PCE obtained was 9.7% , photocurrent density ( $J_{sc}$ ) of  $17.6 \text{ mA/cm}^2$ , and open-circuit voltage ( $V_{oc}$ ) of 888 mV (Naam Gyu Park, 2015). In this type of structure the hole transport material was infiltrated inside the mesoporous oxide layer. In another work by (Rahul et al., 2017) the sandwich structured perovskite solar cells were fabricated at room temperature without the HTM, in the presence of solid polymer electrolyte. The flow chart and mechanism of the sandwich structured perovskite solar cell used in the present work is demonstrated as under in figure 3.

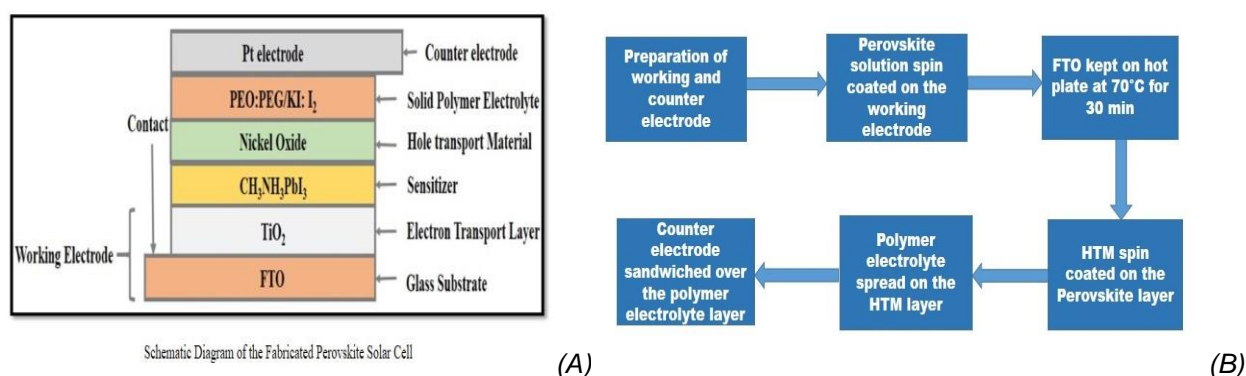


Figure 3. (A) Flowchart and (B) schematic diagram of Sandwich structured Perovskite solar cell

As shown in the figure 3, the fabrication of the perovskite solar cell, requires a working electrode and a counter electrode, blocking layer, electron transport layer, hole transport layer, PEO:PEG based solid polymer electrolyte and the perovskite material. As we know the working of a solar cell is based on three basic phenomenon i.e. charge generation, charge separation and charge collection. In the case of perovskite solar cell charge generation is absorption coefficient (Assadi et al., 2018), it absorbs the radiations, its bound electrons in highest occupied molecular orbital (HOMO) absorb this energy and move to the lowest unoccupied molecular orbital (LUMO) of the

perovskite cell. The electron transport layer, in the present research work specifically  $\text{TiO}_2$ . The photo-excited electrons produced in this process are injected in the conduction band of electron transport layer  $\text{TiO}_2$  which is referred to as charge separation process. The same procedure follows for the holes which are created in the HOMO of the perovskite layer, similarly through the HTM the holes are separated and transported further. The photo-injected electrons are transported through the porous  $\text{TiO}_2$  and holes are transported through the HTM (organic or inorganic) and they get eventually collected on FTO and transported through the outer circuit to give photo current. The

role of solid polymer electrolyte is also very crucial in the sandwich structured solar cells as they aid in efficient charge transfer to the respective electrode. They also acts as a means to regenerate the sensitizer material (Srivastava et al.,2022). They also contribute in having a better contact between the hole transport material and the platinum electrode especially in the sandwich structured solar cell.

### 3.1. Synthesis of Processes involved in the PSC

#### 3.1.1. Material Synthesis

For the preparation of hybrid organic inorganic lead based perovskite material  $\text{MAPbI}_3$ , we first prepare methyl ammonium iodide (MAI) by mixing 20 ml HI and 20 ml Methylamine in a round bottom flask under ice bath treatment (Srivastava et al., 2021) for two hours. The solution prepared is kept in vacuum oven at  $60^\circ\text{C}$  for 24 hours. The yellow color precipitate is washed thoroughly with diethyl ether until a white colour precipitate is formed. Once MAI is prepared, it is mixed with an equal molar ratio of 1:1 with  $\text{PbI}_2$  in N, N-Dimethyl Formamide (DMF) and stirred continuously for 6 hours at  $60^\circ\text{C}$  to obtain a yellow colour perovskite ( $\text{MAPbI}_3$ ) solution.

#### 3.1.2. Preparation of working and the counter electrode

The Working (WE) and counter electrode (CE) are two crucial parts of the PSC for its laboratory scale preparation. For this, we take the FTOs of size of  $1.5 \times 1.5 \text{ cm}^2$ , for cleaning of FTOs, they are sonicated in water and then in Acetone for three hours respectively. For WE, the FTO is coated with blocking layer (BL) Ti(IV) bis(ethyl acetoacetato)-diisopropoxide solution (2 wt% in 1-butanol) is applied and by the spin coating method it is evenly spread over the surface of glass substrate (leaving contact area with help of a scotch tape) and annealed at  $500^\circ\text{C}$  for 30 min in a muffle furnace (Xu et al., 2016, El Henawey et al., 2016). After this blocking layer coated with FTO, is covered with two layers of scotch tape at both ends, then porous  $\text{TiO}_2$  is applied to it by the Doctor Blading method. After applying  $\text{TiO}_2$ , the FTO is sintered at  $500^\circ\text{C}$  for 30 min. A porous  $\text{TiO}_2$  film of  $10 \mu\text{m}$  with pore diameter of 10-15 nm is obtained because of the sintering process. For the counter electrode the solar cell is prepared by spin coating then sintering at  $500^\circ\text{C}$  of a thin layer of  $\text{H}_2\text{PtCl}_6$  on another piece of FTO-coated glass substrate (Yang et al. 2015). The polymer electrolyte which is specifically used in the present research work is the solid polymer electrolyte, which is prepared by dissolving

polyethylene oxide (PEO) and polyethylene glycol (PEG) and the redox couple i.e., 10% KI and  $\text{I}_2$  (10% of KI) in 5 ml of acetonitrile. The solution is stirred continuously for 3-4 days until a homogeneous solution is prepared.

### 3.2. Fabrication Process:

#### 3.2.1. Fabrication of the PSC

The fabrication of the PSC includes the following essential components: first is the Fluorine doped Tin oxide (FTO) coated glass substrate. Second, porous, nanocrystalline semiconducting  $\text{TiO}_2$  for working electrode, third is the coating of  $\text{MAPbI}_3$  perovskite sensitizer, fourth is the hole transport material (HTM), fifth is a secondary component i.e. polymer electrolyte and sixth is ( $\text{H}_2\text{PtCl}_6$ ) platinum coated counter electrode. The method to prepare the working and the counter electrode has already been discussed in the previous section. The  $\text{MAPbI}_3$  perovskite material and the inorganic HTMs have been synthesised in the laboratory. The perovskite solution is deposited through spin coating on the mesoporous layer of  $\text{TiO}_2$  on the glass substrate and is then placed on hot plate for 30 min at  $70^\circ\text{C}$ . The HTM is then drop casted on the perovskite layer. The final step of fabrication consists of sandwiching the counter electrode on the working electrode (fig. 3 B).

## 4. RESULT AND DISCUSSION

### 4.1. $\text{MAPbI}_3$ based Perovskite Solar Cell

When the  $\text{CH}_3\text{NH}_3\text{PbI}_3$  sample is examined in daylight, a yellow colour solution is visible. Under UV light at a shorter wavelength (254 nm), the same solution emits a green colour (Fig. 4) radiation, which corresponds to 550 nanometers, in value. It indicates that photons absorb light at shorter wavelengths and radiate at longer wavelengths. This implies the presence of fluorescence in the perovskite material. The absorbance curve shows that there is a slight peak at 530 nm, which is followed by a sharp rise in the curve. The band gap energy  $E_g$ , according to the figure, 4 (b) is 2.78 eV. The surface morphology of the perovskite surface is described by SEM analysis of a thin film of the material on a glass sheet. Figure. The SEM image of the  $\text{CH}_3\text{NH}_3\text{PbI}_3$  thin film is shown in Figure 4(d) below, which also features flowery islands with a rod-like structure. These features demonstrate the crystalline behavior of methyl ammonium lead iodide-based perovskites, as suggested by their structural description. It establishes the porous nature of the perovskite film when magnified to a higher degree.

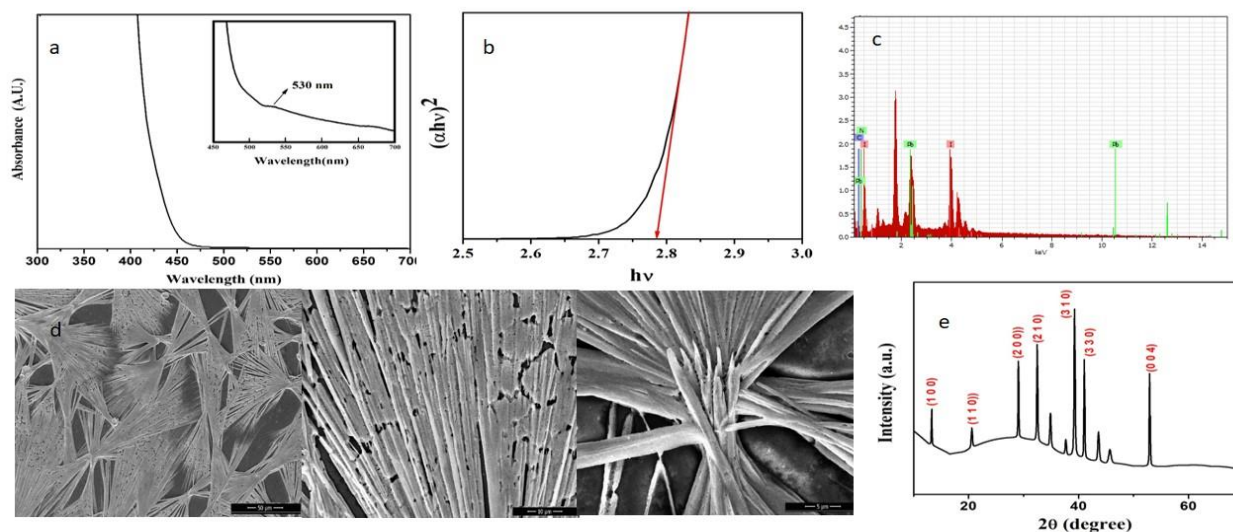


Figure 4. (a) UV absorbance curve of  $\text{MAPbI}_3$  (b) Tauc's plot of  $\text{MAPbI}_3$  (c) EDX Analysis of  $\text{MAPbI}_3$  (d) SEM images of  $\text{MAPbI}_3$  (e) XRD of  $\text{MAPbI}_3$

This makes it more likely for HTM to permeate the perovskite material and improve the interface. The  $\text{MAPbI}_3$  rod-shaped structures, as demonstrated, are advantageous for effective charge transfer applications and superior light harvesting because these rods can actually absorb both the surrounding wave and the portion of a wave that is incident directly on them. According to earlier research, the perovskite solution coated on FTO using the spin coating method has a rod-shaped structure, which means that the FTO substrate is not completely covered. This is explained by the fact that methyl ammonium iodide and lead iodide have different solubilities (Ahn et al., 2015; Park Naam Gyu (2016)). Due to the variance in crystal growth rate caused by the evaporation of the solvent DMF and the high solubility of MAI and low solubility of lead iodide, this can occasionally result in poor morphology. The perovskite EDX image, as shown in . Figure 4(c), amply demonstrates the presence of each component i. E. , lead (Pb), nitrogen (N), carbon (c), and iodine (I). However, the fact that DMF was used as the solvent for the perovskite material also indicates the presence of oxygen. The elemental composition of perovskite contains oxygen due to the fact that DMF has a boiling point of 153 °C and can be heated to 70 °C when spin-coated. The methyl ammonium lead iodide structural characteristics are determined by the XRD measurements (Fig. 4 e). Using Scherer's formula and the XRD pattern, the crystallite size was determined to be 45.82 nm. Significant peaks are visible in the perovskite material's XRD pattern at

13.26°, 20.56°, 29.03°, 32.45°, 39.25°, 41.05°, and 52.91°. These peaks are in close agreement with peaks previously reported (Rajamanickam et al. 2016.). These 2θ values represent (1 0 0), (1 1 0), (2 0 0), (2 1 0), (3 1 0), (3 3 0), and (0 0 4), in that order. This suggests that  $\text{MAPbI}_3$  has a cubical structure. Nevertheless, it also implies that the perovskite material undergoes a phase transition from a tetragonal to a cubic crystal structure at 330.4 K, or roughly 67°C (Baikie et al. 2013, as the perovskite solution is heated to 70°C after being spin coated on the FTO, potentially resulting in a phase transition in the perovskites. In the XRD pattern, a hump that ranges from 2θ= 20° to 2θ= 35° is clearly visible.

#### 4.2. PSC using organic Hole transport Material

Numerous studies have been conducted on the production of PSC with organic hole transport materials. Hole transporting materials (HTMs) are primarily used in devices to make it easier for holes to gather and move after being injected from the light harvester. This helps to ensure that electrons and holes are effectively separated. For perovskite solar cells (PSCs) to function properly, this procedure is essential. HTMs need to possess specific qualities in order to achieve high-performing PSCs. These qualities include: (1) proper HOMO levels that align with the valence band energy (VBE) of perovskite materials, which is essential for hole injection and transport across different interfaces; (2) notable hole mobility and resistance to photochemical degradation; and (3) the capacity to dissolve well in organic solvents.

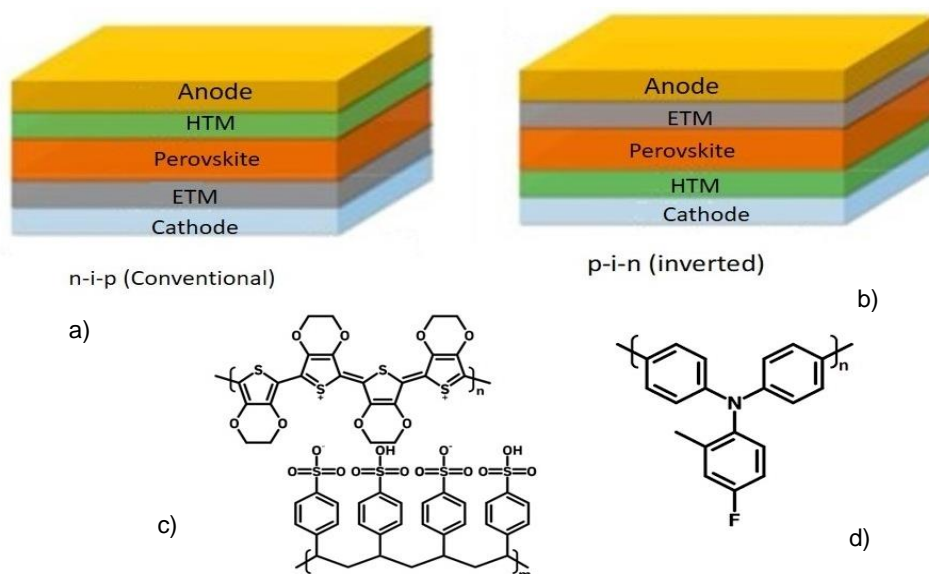


Figure 5. Solid-state perovskite solar cells typically have two device structures as shown in: (a) an inverted planar heterojunction structure and (b) a conventional planar heterojunction structure (c) Widely used organic HTMs have molecular structures as shown in figure 5. (Fu et al., 2022)

As of now 2,2',7,7'-Tetrakis[N,N-di(4-methoxyphenyl) amino]-9,9'-spirobifluorene (spiro-OMeTAD) is recognized as one of the most effective HTMs in perovskite solar cells (PSCs) due to its fulfilment of many previously mentioned criteria. Historically, Spiro-OMeTAD has been employed as a functional transport material in both light emitting diodes and dye-sensitized solar cells, with extensive efforts made towards optimizing its composition and characteristics. Despite its advantages, the high cost of Spiro-OMeTAD, attributed to its complex synthesis process, the need for costly sublimation steps, and the use of toxic and corrosive chemicals, significantly hampers its potential for widespread application in the future (Fu et al., 2022). Currently, 2,2',7,7'-Tetrakis[N,N-di(4-methoxyphenyl)amino]-9,9'-spirobifluorene (spiro-OMeTAD) stands out as a highly efficient HTM in perovskite solar cells (PSCs), meeting many of the essential requirements previously described. In the past, spiro-OMeTAD has served as an effective transport material in technologies such as light emitting diodes and dye-sensitized solar cells, with significant optimization of its formula and properties undertaken. However, its widespread adoption is hindered by the prohibitive cost, roughly 500 euros per gram, which is a consequence of its complicated production process, expensive sublimation procedures, and the employment of hazardous and corrosive substances.

#### 4.3. Perovskite Solar Cells performance with PEDOT:PSS as HTM

To fabricate the perovskite layer, two separate solutions were prepared. Initially, a solution of  $\text{PbI}_2$  in DMF with a density of 462 mg/mL was made,

alongside a solution of  $\text{CH}_3\text{NH}_3\text{I}$  in isopropanol at a density of 10 mg/mL. The  $\text{PbI}_2$  solution was then applied to the working electrode by spin-coating at a speed of 1000 rpm for a duration of 60 seconds. Following this, the FTO glass coated with the yellow  $\text{PbI}_2$  film was dipped into the  $\text{CH}_3\text{NH}_3\text{I}$  solution for 20 seconds, which changed its color to dark brown. Afterwards, this FTO glass, now coated with the perovskite film, was heated at 70°C for 30 minutes on a hot plate.

Then, 20 mL of PEDOT:PSS, which acts as an efficient hole transport material, was deposited on the perovskite film using the drop-casting method. The counter electrode was produced by applying an  $\text{H}_2\text{PtCl}_6$  solution to a separate piece of FTO glass via spin-coating, followed by annealing it at 500°C for 30 minutes. This platinum counter electrode was then positioned atop the working electrode, culminating in the creation of a sandwich structure. The assembly of this perovskite solar cell was carried out in ambient conditions, where the temperature stood at 35°C and the relative humidity at 69%.

#### 4.4. Fabrication of PSC using Inorganic HTMs

Inorganic compounds with effective band gap compatibility, suitable conductivity have proved to be a replacement for the organic HTMs in the PSCs. One of the effective HTM is copper thiocyanate  $\text{CuSCN}$ . Qin and colleagues pioneered the use of copper thiocyanate ( $\text{CuSCN}$ ) as a hole transport material (HTM) in the construction of PSCs. They observed that solar cells incorporating  $\text{CuSCN}$  as an HTM demonstrated a PCE of 12.4% under 1 sun condition, compared to 6.7%.

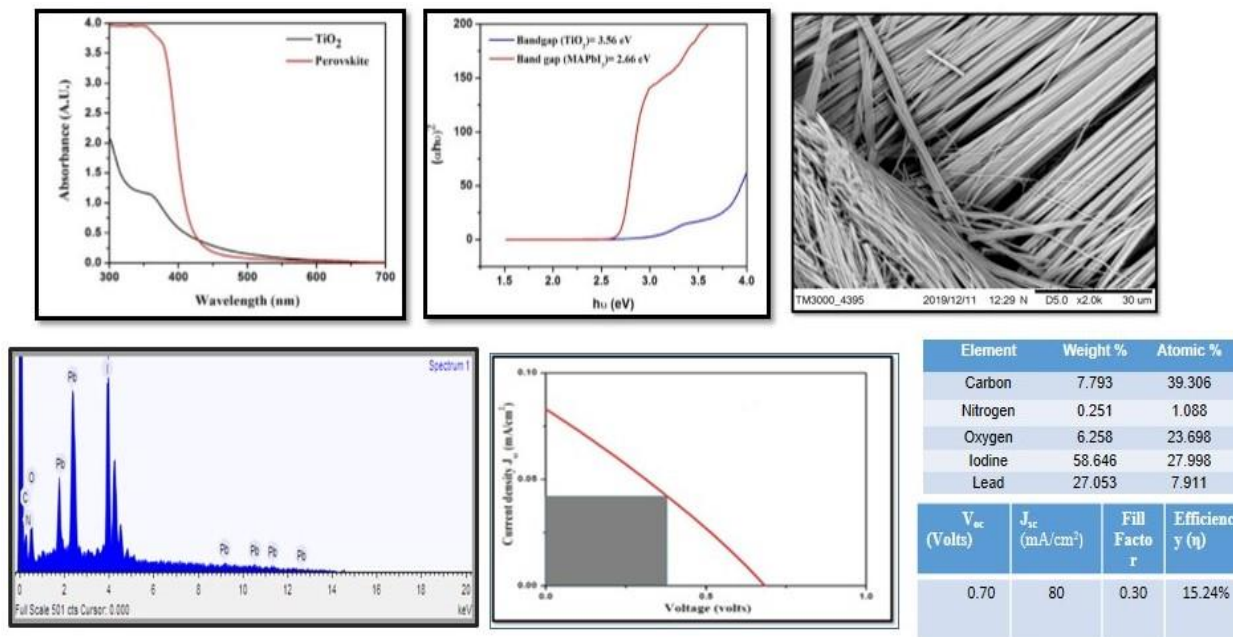


Figure 6. (A) and (B) represents the absorbance and bandgap of two step deposition of MAPbI<sub>3</sub>. (C) represents the EDAX of MAPbI<sub>3</sub> (D) PCE curve of PSC using PEDOT:PSS as HTM

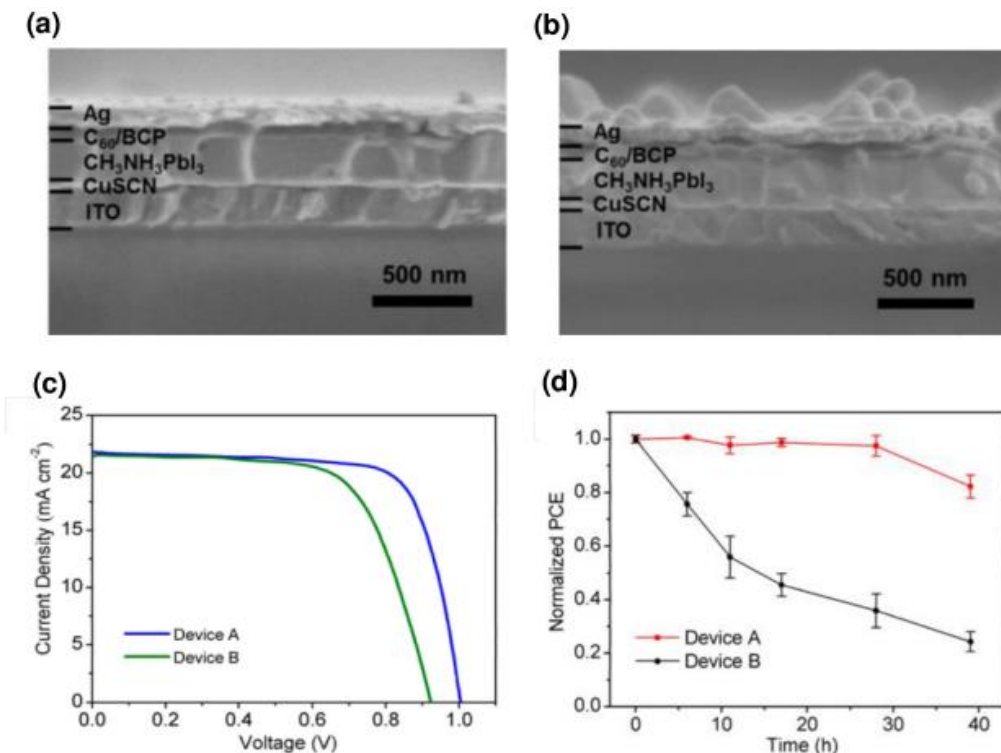


Figure 7. Cross-sectional pictures of SEM showing the PSC, with the one-step fast deposition-crystallization method (Device A) (a) and (b) two-step sequential deposition process (Device B). (c) JV characteristics of Devices A and B under AM 1.5G 100 mW/cm<sup>2</sup> simulated sunlight at a scan rate of 0.5 V s<sup>-1</sup> (d) The corresponding IPCE spectra of Devices A and B. (Ye et al., 2015)

For cells without CuSCN. The incident photon-to-current efficiency (IPCE) spectra indicated that the inclusion of CuSCN HTM enhances internal

quantum efficiency, along with more effective charge injection and collection in PSCs. These findings underscore the potential of CuSCN as an



effective and affordable HTM option for PSCs. Following this, Ye and colleagues showed that inverted planar PSCs utilizing CuSCN HTM achieve a PCE of 16.6%, rivaling traditional cells that use organic hole conductors. These devices, constructed with high-quality  $\text{CH}_3\text{NH}_3\text{PbI}_3$  films atop a CuSCN layer through a rapid one-step deposition-crystallization method (referred to as Device A), have smoother surfaces and less interfacial contact resistance between the perovskite layer and the selective contacts. This was in sharp contrast to films produced using a two-step sequential deposition process (referred to as Device B) (Figure 7).

Nickel oxide is another common inorganic HTM. Strong environmental stability, a broad band gap, of 5.4 eV, and a valence band (VB) that closely resembles that of perovskite are some of its distinguishing features. Because of these characteristics, NiOx can be used in place of the organic PEDOT:PSS HTMs in PSCs. The

application of a NiO interlayer as a HTM in a planar heterojunction solar cell was demonstrated by Jeng and colleagues. PCBM ([6,6]-phenyl C61-butyric acid methyl ester) was used as the electron transport layer. The PCE of this configuration was 71.8 %, which is significantly higher than 30.9 % PCE of devices that use the organic HTM PEDOT:PSS. Because of the better energy band levelling between the NiO and the perovskite light absorber, the performance is improved. Wang et al. demonstrated in a different study the efficiency of organo-metallic inverted hybrid PSCs, attaining a PCE of 9.51%. As a p-type electrode material within the PSC, this study used mesoscopic NiOx in nanocrystalline form, which improved charge transport at the NiOx/perovskite interface. With an open-circuit voltage (Voc) of [6,6]-phenyl C61-butyric acid methyl ester, mesoscopic NiOx, perovskite, and PCBM (p-i-n active layer structure), the device's photovoltaic parameters were noteworthy.

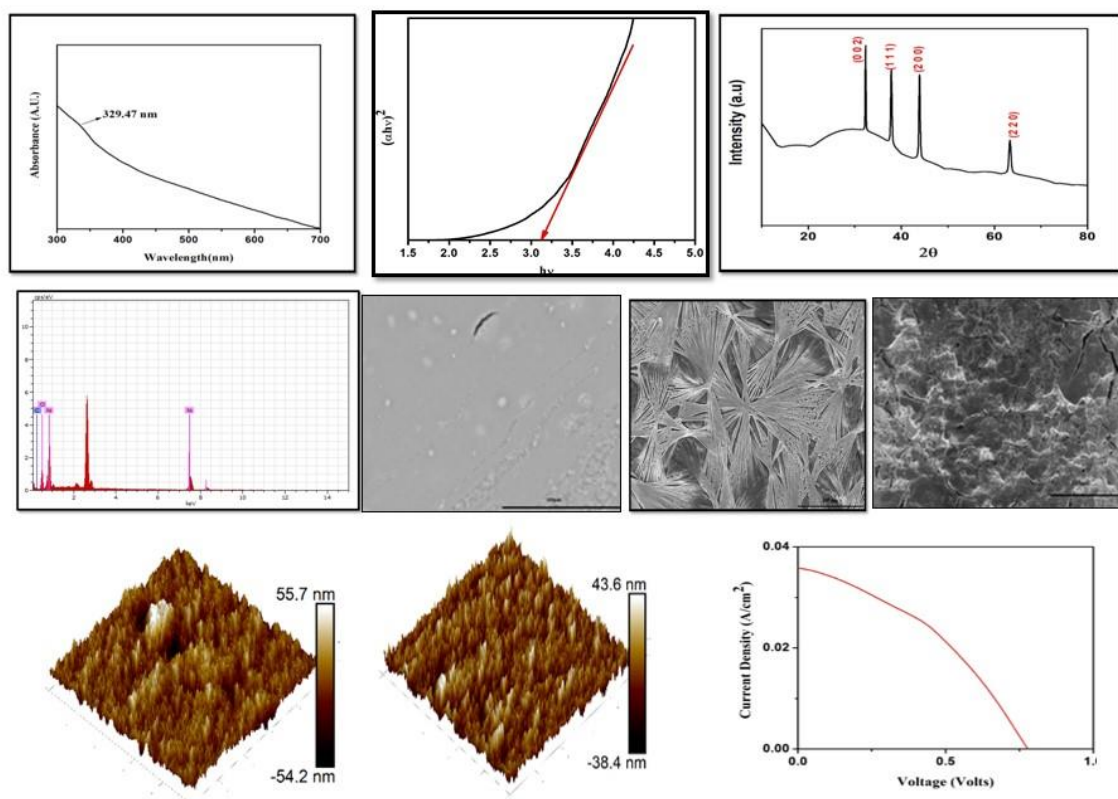


Figure 8. Representation of the various characteristics features of NiO and PCE graph

CuI stands out as a highly effective, cost-efficient, stable, wide bandgap semiconductor with notable conductivity, making it an excellent choice for use as a HTM in PSCs. Christians and colleagues engineered PSCs utilizing CuI as the HTM through a drop-casting technique, achieving a PCE of 6% alongside remarkable photocurrent stability. Through impedance spectroscopy, it was

discovered that CuI-based cells exhibit electrical conductivity that is two orders of magnitude higher than that of cells using spiro-OMeTAD as the HTM, which significantly enhances the fill factor (FF) values.

Further, stability assessments comparing CuI and spiro-OMeTAD-based solar cells revealed that CuI solar cells maintained a consistent current,

whereas the spiro-OMeTAD cells experienced a reduction in short-circuit current density ( $J_{sc}$ ) by about 10%, as illustrated in This evaluation was conducted under continuous 100 mW/cm<sup>2</sup> AM 1.5G illumination for 2 hours without encapsulation in ambient conditions. One of the studies uses a sandwich configuration to study the synthesis of polymer electrolyte and hole transport material (HTM) and their application in a PSC in a standard room environment. Solution-processed spin-coating was used to assemble a planar structure made of WE/TiO<sub>2</sub>/CH<sub>3</sub>NH<sub>3</sub>PbI<sub>3</sub>/HTM/electrolyte/CE. With an open-circuit voltage ( $V_{oc}$ ) of 0.63 V, a short-circuit current density ( $J_{sc}$ ) of 33 mA/cm<sup>2</sup>, and a fill factor of 0.65, the PSC's electrical

performance was assessed using a solar simulator. The results showed an efficiency of 13.64 percent (Figure 9). This research highlights the innovative aspect of fabricating a sandwich-structured PSC in ambient conditions with a notably high efficiency (Srivastava et al., 2023). Various research work is going on, in the field of bifacial perovskite solar cells where Cu doped NiO is used as a hole transport material. In such type of solar cells, the single walled CNTs (carbon nano tubes) are used as both front and back electrodes which offers high transparency, conductivity and stability. Such type of cells are capable of generating high power density of 36% (Zhang et al., 2024 )

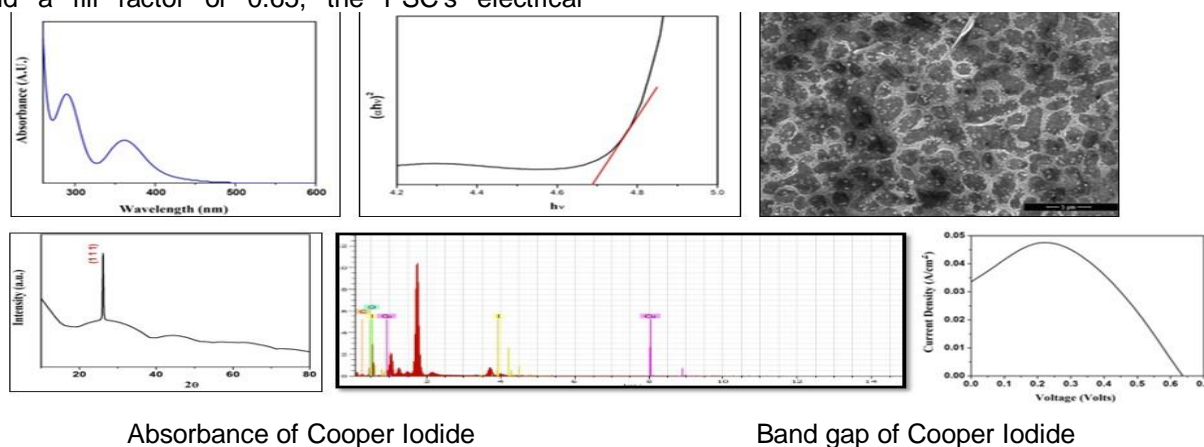


Figure 9. Representation of the various characteristics features of CuI and PCE.graph

## 5. CONCLUSION

This paper addresses various scalable techniques for the fabrication of various functional layers of a PSC. It also clarifies the techniques used in the deposition process plays a very crucial role in enhancing the efficiency and stability of the PSC. It signifies the fact that HTM characteristics are intimately linked to a number of variables, such as molecular stacking, energy levels, hole mobility, and film-forming capabilities. To maximize the performance of HTMs, it is imperative to thoroughly take into account the effects of a number of factors. Two of the most important PSC concerns to take into account are lowering the price of solar cells and enhancing their stability for possible uses. Inorganic HTMs that are affordable, easily synthesized, extremely stable, long-lasting, and transparent (both in the visible and near-IR range) are used in this article to address these problems. In addition, fabrication costs are less than those of organic HTMs. The highest PCE of 19 % and 16.6 % was recently recorded by copper-based inorganic HTMs such as CuO and CuSCN in PSCs. Thus, by altering the morphology of the perovskite film, mixing organic and inorganic

materials, altering the deposition processes, and changing the metal oxides, PSCs' power conversion efficiency and stability were increased. Furthermore, it was discovered that inorganic HTMs were more economically feasible than organic HTMs.

### Acknowledgement

We are extremely thankful to Seed Fund (SU/SF/2023/02) provided by Sharda University to support this research.

## 6. REFERENCES

- [1] U.EIA (2015) Analysis of the impacts of the Clean Power Plan, US Energy Information Administration, Washington DC, pp.1-96.
- [2] M.A.McGeoch, S.H. Butchart, D. Spear, E. Marais, E. Kleyhans, A. Symes, J.Chanson, M. Hoffmann (2010) Global indicators of biological invasion: species numbers, biodiversity impact and policy responses, Diversity and Distributions, 16(1), 95-108. <http://doi/10.1111/j.1472-4642.2009.00633.x>
- [3] R.F.Service (2005) Solar energy. Is it time to shoot for the sun?, Science (New York, NY), 309(5734), 548-551. <http://doi/10.1126/science.309.5734.548>.

- [4] H. Şengül, T. L. Theis, (2011)., An environmental impact assessment of quantum dot photovoltaics (QDPV) from raw material acquisition through use. *Journal of Cleaner Production*, 19(1), 21-31. <http://doi/10.1016/j.jclepro.2010.08.010>.
- [5] M. Grätzel, (2009)., Recent advances in sensitized mesoscopic solar cells. *Accounts of chemical research*, 42(11), 1788-1798. <https://doi.org/10.1021/ar900141y>.
- [6] P.Roy, A.Ghosh, F.Barclay, A.Khare, E.Cuce (2022) Perovskite solar cells: a review of the recent advances. *Coatings*, 12(8), 1089. <https://doi.org/10.3390/coatings12081089>.
- [7] K.Nishimura, M. Amarudin, D.Hirotnani, K Hamada, Q. Shen, S. Iikubo,S.Hayase (2020) Lead-free tin-halide perovskite solar cells with 13% efficiency. *Nano Energy*, 74, 104858. <https://doi.org/10.1016/j.nanoen.2020.104858>.
- [8] A. Kojima, K. Teshima, Y. Shirai, T. Miyasaka (2009) Organometal halide perovskites as visible-light sensitizers for photovoltaic cells. *Journal of the American chemical society*, 131(17), 6050-6051. <https://doi.org/10.1021/ja809598r>.
- [9] H.S. Kim, C. R. Lee, J.H. Im, K.B. Lee, T. Moehl, A. Marchioro, N. G. Park (2012) Lead iodide perovskite sensitized all-solid-state submicron thin film mesoscopic solar cell with efficiency exceeding 9%. *Scientific reports*, 2(1), 591. <http://doi/10.1038/srep00591>.
- [10] J. W. Lee, H.S. Kim, N. G. Park (2016) Lewis acid–base adduct approach for high efficiency perovskite solar cells. *Accounts of chemical research*, 49(2), 311-319. <https://doi.org/10.1021/acs.accounts.5b00440>.
- [11] T. Baikie, Y. Fang, J. M. Kadro, M. Schreyer, F. Wei, S. G. Mhaisalkar, T. White (2013) Synthesis and crystal chemistry of the hybrid perovskite (CH<sub>3</sub>NH<sub>3</sub>)PbI<sub>3</sub> for solid-state sensitised solar cell applications. *Journal of Materials Chemistry A*, 1(18), 5628-5641. doi: <https://doi.org/10.1039/C3TA10518K>.
- [12] Q. Dong, Y. Fang, Y. Shao, P. Mulligan, J. Qiu, L. Cao, J. Huang, (2015) Electron-hole diffusion lengths > 175 µm in solution-grown CH<sub>3</sub>NH<sub>3</sub>PbI<sub>3</sub> single crystals. *Science*, 347(6225), 967-970. <https://doi.org/10.1126/science.aaa5760>.
- [13] Jr. Ponceca, T.J. Savenije, M. Abdellah, K. Zheng, A. Yartsev, T. Pascher, V. Sundström (2014) Organometal halide perovskite solar cell materials rationalized: ultrafast charge generation, high and microsecond-long balanced mobilities, and slow recombination. *Journal of the American Chemical Society*, 136(14), 5189-5192. <https://doi.org/10.1021/ja412583t>.
- [14] M.K. Assadi, S. Bakhoda, R. Saidur, H. Hanaei (2018) Recent progress in perovskite solar cells. *Renewable and Sustainable Energy Reviews*, 81, 2812-2822. <https://doi.org/10.1016/j.rser.2017.06.088>
- [15] D. B. Mitzi, M.T. Prikas, K. Chondroudis (1999) Thin film deposition of organic– inorganic hybrid materials using a single source thermal ablation technique. *Chemistry of materials*, 11(3), 542-544. <https://doi.org/10.1021/cm9811139>.
- [16] M.M Lee, J. Teuscher, T. Miyasaka, T.N. Murakami, H.J. Snaith (2012) Efficient hybrid solar cells based on meso-structured organometal halide perovskites. *science*, 338(6107), 643-647. <https://doi.org/10.1021/cm9811139>
- [17] G. Longo, C. Momblona, M.G. La-Placa, L. Gil-Escrig, M. Sessolo, H. J. Bolink, (2017) Fully vacuum-processed wide band gap mixed-halide perovskite solar cells. *ACS energy letters*, 3(1), 214-219. <https://doi.org/10.1021/acseenergylett.7b01217>
- [18] A. M. Igual-Muñoz, J. Ávila, P.P. Boix, H. J. Bolink (2020) FAPb<sub>0.5</sub>Sn<sub>0.5</sub>I<sub>3</sub>: A narrow bandgap perovskite synthesized through evaporation methods for solar cell applications. *Solar RRL*, 4(2), 1900283. <https://doi.org/10.1002/solr.202070024>
- [19] Y.H. Chiang, M. Anaya, S. D. Stranks (2020) Multisource vacuum deposition of methylammonium-free perovskite solar cells. *ACS Energy Letters*, 5(8), 2498-2504. <https://doi.org/10.1021/acsenergylett.0c00839>
- [20] J. Feng, Y. Jiao, H. Wang, X. Zhu, Y. Sun, M. Du, Y. Cao, D. Yang, S.F. Liu (2021) High-throughput large-area vacuum deposition for high-performance formamidinium-based perovskite solar cells, *Energy & Environmental Science*, 14(5), 3035-3043. doi: 10.1039/D1EE00656Ka.
- [21] J. Li, H. Wang, X.Y. Chin, H.A. Dewi, K. Vergeer, T.W. Goh, J.W.M. Lim, J.H. Lew, K.P. Loh, C. Soci, T.C. Sum (2020) Highly efficient thermally co-evaporated perovskite solar cells and mini-modules, *Joule*, 4(5), 1035-1053. doi: 10.1016/j.joule.2020.03.007.
- [22] P. Zhang, M. Li, W.C. Chen (2022) A perspective on perovskite solar cells: emergence, progress, and commercialization, *Frontiers in Chemistry*, 10, 802890. doi: 10.3389/fchem.2022.802890.
- [23] N.J. Jeon, J.H. Noh, Y.C. Kim, W.S. Yang, S. Ryu, S.I. Seok (2014) Solvent Engineering for High-Performance Inorganic–Organic Hybrid Perovskite Solar Cells, *Nature Materials*, 13(9), 897-903. doi: 10.1038/nmat4014.
- [24] D. Bi, C. Yi, J. Luo, J.D. Décoppet, F. Zhang, S.M. Zakeeruddin, X. Li, A. Hagfeldt, M. Grätzel (2016) Polymer-templated nucleation and crystal growth of perovskite films for solar cells with efficiency greater than 21%, *Nature Energy*, 1(10), 1-5. doi: 10.1038/nenergy.2016.189.
- [25] Y. Gao, L. Yang, F. Wang, Y. Sui, Y. Sun, M. Wei, J. Cao, H. Liu (2018) Anti-solvent surface engineering via diethyl ether to enhance the photovoltaic conversion efficiency of perovskite solar cells to 18.76%, *Superlattices and Microstructures*, 113, 761-768. <https://doi.org/10.1016/j.spmi.2017.12.014>

- [26] Y. Wu, X. Yang, W. Chen, Y. Yue, M. Cai, F. Xie, E. Bi, A. Islam, L. Han (2016) Perovskite solar cells with 18.21% efficiency and area over 1 cm<sup>2</sup> fabricated by heterojunction engineering, *Nature Energy*, 1(11), 1-7.  
<https://doi.org/10.1038/nenergy.2016.215>
- [27] P.L. Qin, G. Yang, Z.W. Ren, S.H. Cheung, S.K. So, L. Chen, J. Hao, J. Hou, G. Li (2018) Stable and efficient organo-metal halide hybrid perovskite solar cells via  $\pi$ -conjugated Lewis base polymer induced trap passivation and charge extraction, *Advanced Materials*, 30(12), 1706126.  
<https://doi.org/10.1002/adma.201706126>.
- [28] M. Srivastava, P.K. Singh, R.C. Singh (2022) Comparative study of PSCs formed by one step and sequential deposition of CH<sub>3</sub>NH<sub>3</sub>PbI<sub>3</sub> using PEDOT: PSS as HTM, *Materials Today: Proceedings*, 49, 3340-3344.  
<https://doi.org/10.1016/j.matpr.2021.03.318>
- [29] C.H. Chiang, M.K. Nazeeruddin, M. Grätzel, C.G. Wu (2017) The synergistic effect of H<sub>2</sub>O and DMF towards stable and 20% efficiency inverted perovskite solar cells, *Energy & Environmental Science*, 10(3), 808-817.  
<https://doi.org/10.1039/C6EE03539H>.
- [30] X. Xu, M. Li, Y.M. Xie, Y. Ma, C. Ma, Y. Cheng, et al. (2019) Porous and Intercrossed PbI<sub>2</sub>-CsI Nanorod Scaffold for Inverted Planar FA-Cs Mixed Cation Perovskite Solar Cells, *ACS Applied Materials & Interfaces*, 11(6), 6126-6135.  
<https://doi.org/10.1021/acsami.8b21835>
- [31] Q. Jiang, L. Zhang, H. Wang, X. Yang, J. Meng, H. Liu, Z. Yin, J. Wu, X. Zhang, J. You (2016) Enhanced electron extraction using SnO<sub>2</sub> for high-efficiency planar-structure HC(NH<sub>2</sub>)<sub>2</sub>PbI<sub>3</sub>-based perovskite solar cells, *Nature Energy*, 2(1), 1-7.  
<https://doi.org/10.1038/nenergy.2016.187>
- [32] J. Zhang, X. Ji, X. Wang, L. Zhang, L. Bi, Z. Su, X. Gao, W. Zhang, L. Shi, G. Guan, A. Abudula (2024) Efficient and Stable Inverted Perovskite Solar Modules Enabled by Solid-Liquid Two-Step Film Formation, *Nano-Micro Letters*, 16, 190-190.  
<https://doi.org/10.1007/s40820-023-00943-6>
- [33] Y. Yoo, G. Seo, H.J. Park, J. Kim, J. Jang, W. Cho, J.H. Kim, J. Shin, J.S. Choi, D. Lee, S.W. Baek (2024) Low-temperature rapid UV sintering of sputtered TiO<sub>2</sub> for flexible perovskite solar modules, *Journal of Materials Chemistry A*, 12(3), 1562-1572.  
<https://doi.org/10.1039/D3TA01474A>
- [34] J. Zhang, X.G. Hu, K. Ji, S. Zhao, D. Liu, B. Li, P.X. Hou, C. Liu, L. Liu, S.D. Stranks, H.M. Cheng (2024) High-performance bifacial perovskite solar cells enabled by single-walled carbon nanotubes, *Nature Communications*, 15(1), 2245.  
<https://doi.org/10.1038/s41467-024-20085-1>
- [35] N.G. Park (2015) Perovskite solar cells: an emerging photovoltaic technology, *Materials Today*, 18(2), 65-72.  
<https://doi.org/10.1016/j.matmod.2014.07.007>.
- [36] P.K. Singh, R. Singh, V. Singh, S.K. Tomar, B. Bhattacharya, Z.H. Khan (2017) Effect of crystal and powder of CH<sub>3</sub>NH<sub>3</sub> on the CH<sub>3</sub>NH<sub>3</sub>PbI<sub>3</sub> based perovskite sensitized solar cell, *Materials Research Bulletin*, 89, 292-296.  
<https://doi.org/10.1016/j.materresbull.2016.12.018>
- [37] M. Srivastava, K. Surana, P.K. Singh, R. Ch (2021) Nickel oxide embedded with polymer electrolyte as efficient hole transport material for perovskite solar cell, *Engineered Science*, 17, 216-223.  
<https://doi.org/10.30919/es8d474>
- [38] Y. Xu, L. Zhu, J. Shi, X. Xu, J. Xiao, J. Dong, H. Wu, Y. Luo, D. Li, Q. Meng (2016) The Effect of Humidity upon the Crystallization Process of Two-Step Spin-Coated Organic-Inorganic Perovskites, *ChemPhysChem*, 17(1), 112-118.  
<https://doi.org/10.1002/cphc.201500928>
- [39] M.I. El-Henawy, R.S. Gebhardt, M.M. El-Tonsy, S. Chaudhary (2016) Organic solvent vapor treatment of lead iodide layers in the two-step sequential deposition of CH<sub>3</sub>NH<sub>3</sub>PbI<sub>3</sub>-based perovskite solar cells, *Journal of Materials Chemistry A*, 4(5), 1947-1952.  
<https://doi.org/10.1039/C5TA08032A>
- [40] N. Ahn, D.Y. Son, I.H. Jang, S.M. Kang, M. Choi, N.G. Park (2015) Highly reproducible perovskite solar cells with average efficiency of 18.3% and best efficiency of 19.7% fabricated via Lewis base adduct of lead (II) iodide, *Journal of the American Chemical Society*, 137(27), 8696-8699.  
<https://doi.org/10.1021/jacs.5b04930>
- [41] N.G. Park, M. Grätzel, T. Miyasaka, K. Zhu, K. Emery (2016) Towards stable and commercially available perovskite solar cells, *Nature Energy*, 1(11), 1-8.  
<https://doi.org/10.1038/nenergy.2016.139>.
- [42] N. Rajamanickam, S. Kumari, V.K. Vendra, B.W. Lavery, J. Spurgeon, T. Druffel, M.K. Sunkara (2016) Stable and durable CH<sub>3</sub>NH<sub>3</sub>PbI<sub>3</sub> perovskite solar cells at ambient conditions, *Nanotechnology*, 27(23), 235404. <https://doi.org/10.1088/0957-4484/27/23/235404>
- [43] T. Baikie, Y. Fang, J.M. Kadro, M. Schreyer, F. Wei, S.G. Mhaisalkar, M. Graetzel, T.J. White (2013) Synthesis and crystal chemistry of the hybrid perovskite (CH<sub>3</sub>NH<sub>3</sub>)PbI<sub>3</sub> for solid-state sensitised solar cell applications, *Journal of Materials Chemistry A*, 1(18), 5628-5641.  
<https://doi.org/10.1039/C3TA10518K>.
- [44] S. Ye, W. Sun, Y. Li, W. Yan, H. Peng, Z. Bian, Z. Liu, C. Huang (2015) CuSCN-based inverted planar perovskite solar cell with an average PCE of 15.6%, *Nano Letters*, 15(6), 3723-3728.  
<https://doi.org/10.1021/acs.nanolett.5b00683>.
- [45] J.Y. Jeng, K.C. Chen, T.Y. Chiang, P.Y. Lin, T.D. Tsai, Y.C. Chang, T.F. Guo, P. Chen, T.C. Wen, Y.J. Hsu (2014) Nickel oxide electrode interlayer in CH<sub>3</sub>NH<sub>3</sub>PbI<sub>3</sub> perovskite/PCBM planar-heterojunction hybrid solar cells, *Advanced Materials*, 26(24), 4107-4113.  
<https://doi.org/10.1002/adma.201400772>

- [46] K.C. Wang, J.Y. Jeng, P.S. Shen, Y.C. Chang, E.W.G. Diau, C.H. Tsai, T.Y. Chao, H.C. Hsu, P.Y. Lin, P. Chen, T.F. Guo (2014) P-type mesoscopic nickel oxide/organometallic perovskite hetero-junction solar cells, *Scientific Reports*, 4(1), 4756. <https://doi.org/10.1038/srep04756>
- [47] Y.Yoo, G.Seo, J.H.Park, J.Kim, J.Jang, H.Cho, J.Kim, J.Shin, J.Choi,D.Lee, W.Baek (2024) Low-temperature rapid UV sintering of sputtered TiO<sub>2</sub> for flexible perovskite solar modules. *Journal of Materials Chemistry A*, 12(3), 1562-1572. <https://doi.org/10.1039/D3TA05666J>

## IZVOD

### SINTEZA I SKALABILNI PROCES ZA PROIZVODNJU PEROVSKITNIH SOLARNIH ČELIJA KORIŠĆENJEM ORGANSKIH I NEORGANSKIH MATERIJALA ZA TRANSPORT RUPA

*Organsko neorganski olovni jodid perovskit materijal se pojavio kao pionir u tome da bude aktivan materijal za treću generaciju solarnih ćelija. Osim sinteze, skalabilni mehanizam koji se koristi za proces depozicije, u velikoj meri utiče na performanse ćelije zahvaljujući svom uticaju na morfologiju, ujednačenu debljinu i interfejs između dva funkcionalna sloja. Ova studija ukratko govori o različitim procesima taloženja uključenim u sastavljanje slojeva solarnih ćelija perovskita (PSC). Materijali za transport rupa (HTM) su ključni deo PSC koji obezbeđuju efikasan transport nosača punjenja. Međutim, efekat organskih i neorganskih HTM je veoma izražen u PSC. Ova studija, takođe, razmatra uticaj organskog i neorganskog HTM na stabilnost i efikasnost sendvič strukturisanog PSC.*

**Ključne reči:** perovskit, solarna energija, PCE, materijal za transport rupa

*Naučni rad*

*Rad primljen: 07.03.2024.*

*Rad korigovan: 23.05.2024.*

*Rad prihvaćen: 06.06.2024.*

Ikhwan Syafiq Mohd Noor

<https://orcid.org/0000-0003-0983-782X>

Muhd Zu Azhan Yahya

<https://orcid.org/0000-0003-1129-0552>